

Theoretical Calculation of Thermochemistry, Energetics, and Kinetics of High-Temperature $\text{Si}_x\text{H}_y\text{O}_z$ Reactions

Michael R. Zachariah* and Wing Tsang

Chemical Science and Technology Laboratory, National Institute of Standards and Technology,
Gaithersburg, Maryland 20899

Received: June 11, 1994; In Final Form: January 3, 1995[®]

Ab-initio molecular orbital calculations have been performed on silicon oxy hydride species and transition states for reactions that may be important to silane combustion and other high-temperature oxidations. Geometries were optimized at both HF/6-31G(d) and MP2/6-31G(d) levels, and vibrational frequencies were calculated at the HF/6-31G(d) level. Heats of formation for both equilibrium and transition state species have been obtained using a bond additivity correction (BAC) procedure at either the MP4/6-31G(d,p)//HF/6-31G(d) or MP4/6-311G(2df,p)//MP2//6-31G(d) level. From the calculated transition state properties, limiting rate expressions have been derived in the usual manner. In the case of unimolecular processes in the broadest sense (decomposition, association, and chemically activated decompositions) RRKM/master equation solutions lead to rate expressions reflecting pressure dependencies.

Introduction

Silane reducing chemistry has received considerable attention due to its importance in semiconductor manufacturing. However, the oxidation side has been subject to relative neglect even though its importance crosses a range of industries. These include microelectronics industries for dielectric coatings, photonics industries from fiber optics manufacture through aerosol processes, and the aerospace industries where silane has been proposed as an ignition source. We note that for all these industries silane's pyrophoric nature makes it a safety hazard, while little is known about the chemical mechanism of oxidation, and an added complexity and an associated interest is that silane oxidation under high supersaturation ratios can rapidly lead to particle nucleation and the attending complexities of two-phase flow with chemistry. Indeed considerable activity has been directed to the issues associated with the formation of silica and silica composites resulting from the gas phase oxidation of silane and other silicon precursors.^{1–5}

One of the major stumbling blocks in the application of chemical knowledge to understanding industrial problems is the lack of reliable thermochemical and kinetic information on silane oxidation in the various regimes encountered. While some effort has been focused on applying analogies with methane combustion chemistry, there are sufficient differences in even the reducing chemistry to suggest that such an approach may lead to substantial errors. Others have applied an empirical approach to obtain thermochemical information for many of the silicon–oxygen intermediates, particularly since no body of experimental data is available.⁶

Ab-initio methods provide a means of addressing these issues. Most recently Schlegel and co-workers⁷ and Lucas et al.⁸ have compiled a substantial database of thermochemistries for the SiH_xO_y system using the G-2 method and reviewed prior calculational results. As a follow-up they have also conducted an ab initio study on the primary reaction pathways leading from the $\text{SiH}_3 + \text{O}_2$ reaction.⁹

This paper represents our initial approach at developing a detailed understanding of silane oxidation leading to particle formation. The specific physical situation is a reactor for the

formation of nanophase SiO/SiO_2 particles. Concentration measurements and some chemical kinetic modeling have been carried out. These have defined the general directions and demonstrated that much more detailed knowledge of the chemistry is required for effective understanding—hence the present effort. The unique feature of the experimental observations is the propensity for oxidation under essentially anaerobic conditions.¹⁰ This absence of molecular oxygen makes necessary the assignment of water vapor as the primary donor of oxygen to silicon species followed by the reaction of these compounds through a variety of pathways. Since direct experimental determinations of the rate expressions for the single-step processes pertaining to such systems are nonexistent and in many cases probably extremely difficult to carry out, we begin our work by using the available tools for estimation, in constructing a framework for more detailed comparisons with experiments.

Method

Molecular orbital calculations were carried out using the GAUSSIAN¹¹ series of programs. Equilibrium geometries were optimized at the HF/6-31g(d) and MP2/6-31(d) levels, and vibrational frequencies and zero-point energies were calculated at the HF/6-31G(d) level using the HF-optimized geometries and scaled by 0.89. Energies were calculated at the MP4/6-311(2df,p) level at the MP2-optimized geometries. In order to obtain reasonable thermochemical data from such a calculation without having to resort to the computational cost of a G2 or higher level theory, a bond additivity correction procedure was implemented. This approach uses the bond additivity correction (BAC) formalism of Melius and co-workers, who have found success applying this correction approach on smaller basis sets.¹² For structures too large to be computed with the large basis set, computations were conducted using the Melius procedure of HF/6-31g(d) geometry optimization and frequencies scaled by 0.89 followed by an energy calculation at the MP4/6-31G(d,p) level.

In the BAC method, errors in the electronic energy of a molecule are treated as bondwise additive and depend on bonding partner and distance. The energy per bond is corrected by calibration at a given level of theory against molecules of

[®] Abstract published in *Advance ACS Abstracts*, March 1, 1995.

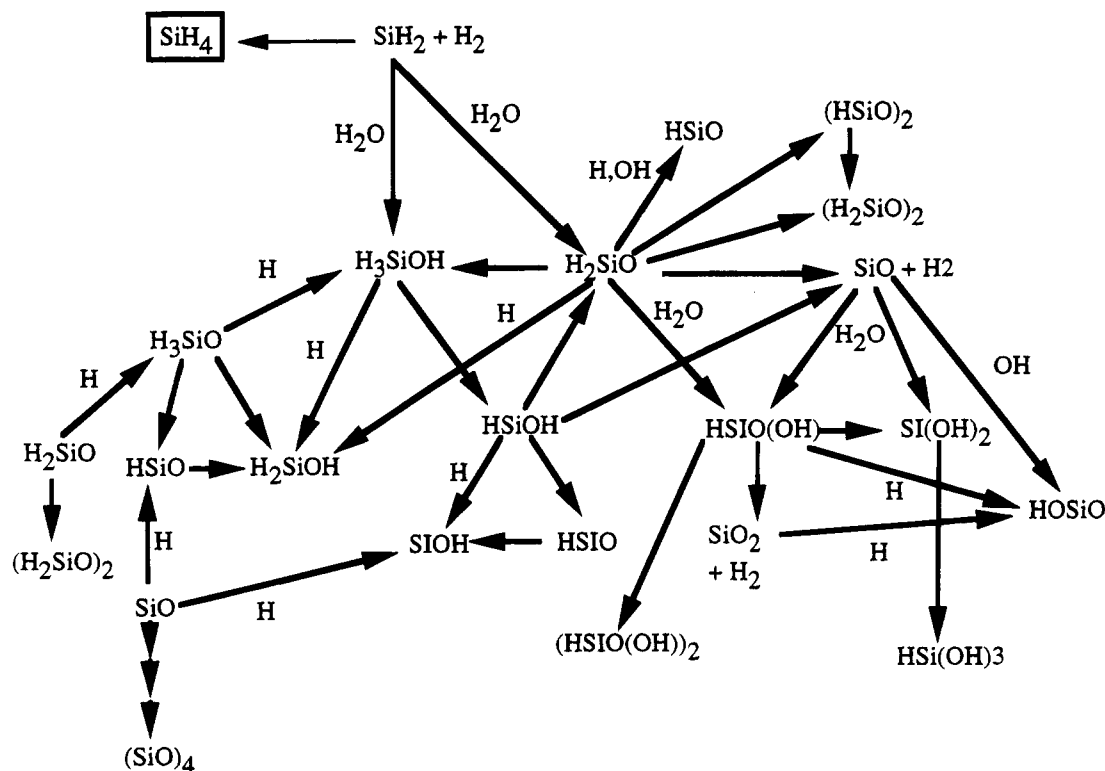


Figure 1. Roadmap of reactions studied. Arrows correspond to exothermic direction.

know energy. Corrections are needed for three types of bonds Si-H, O-H, and Si-O. SiH₄ and H₂O were used for the Si-H and O-H bonds, respectively. Since no experimental data are readily available to calibrate the Si-O bond, we used the G2 values computed for SiH₂O and SiH₃OH (ref 7 and this work).

Corrections are made using a function that decays exponentially away with increasing bond distance (r_{ij})

$$E_{\text{BAC}}(A_i - A_j) = A_{ij} \exp(-\alpha_{ij} r_{ij}) \quad (1)$$

where A_{ij} and α_{ij} are calibration constants for

bond	calibration species	MP4/6-311(2df,p)// MP2/6-31(d)		MP4/6-31G(d,p)// HF/6-31G(d)	
		A_{ij}	α_{ij}	A_{ij}	α_{ij}
Si-H	SiH ₄	38.8	2.0	92.8	2.0
O-H	H ₂ O	45.8	2.0	72.4	2.0
Si-O	SiH ₂ O, SiH ₃ OH	562.4	3.15	628.3	2.42

For open-shelled molecules an additional correction is needed due to contamination from higher spin states. This error is estimated using an approach developed by Schlegel in which the spin energy correction is obtained from¹³

$$E_{\text{spin}} = E(\text{UMP3}) - E(\text{PUMP3}) \quad (2)$$

The calculated properties for the transition state can readily be converted to rate constants for true bimolecular and unimolecular thermal processes using standard relationships.¹⁴ In cases where energy at the transition state geometry was lower than that of the reactant or product, the reaction was assumed to proceed without an energy barrier. An added complication is the possible pressure dependence of the unimolecular process. RRKM theory provides a framework for treating such situations.¹⁵ The reference to "true" bimolecular reactions relegates this class of process to abstractions and to association reactions in the high-pressure limit. Other bimolecular reactions which result in the formation of hot molecules can be and are treated

within the RRKM theory. Pressure dependence is a manifestation of energy transfer effects and is treated through solution of the steady state relations of the master equation. This approach leads itself naturally to the treatment of reactions with multiple channels. The key parameter in such a treatment is the step size down, which we have assumed using the relation step size down = temperature/3 cm⁻¹, assuming N₂ is the collision partner. This is in accord with observations for many organic systems.^{16,17} Although one does not expect drastic changes, especially at the temperatures of this application, there is a need to obtain such information for silicon systems.

In calculating chemical activation effects, we have considered endothermic as well as exothermic channels. At the temperatures of interest the usual neglect of the former is not justified in view of the very broad distribution functions. A serious problem in the present treatment is our inability to properly include effects arising from isomerization processes. For these processes the excited molecules are not removed from consideration upon passage across the reactive barrier. This is not a serious situation if the isomerization is very exothermic, since recrossing rates will be small. Conversely, if the reaction is very endothermic, recrossings will be very large. We have used this as a criterion for considering or neglecting isomerization. In practical terms this means that in the endothermic case the contribution from the alternative channels will be maximized, while in the other case it will be minimized. This is probably sufficient for the present rough treatment. Should these turn out to be key processes through sensitivity analysis, then a more careful treatment will probably be appropriate. For the reactions without a barrier we have assumed combination rate constants (at the high-pressure limit) on the order of 1×10^{14} cm³ mol⁻¹ s⁻¹ for reactions involving H atoms and 2×10^{13} cm³ mol⁻¹ s⁻¹ for those involving polyatomic species. Transition state structures are then derived on the basis of the A-factor that is calculated from detailed balance, which in all cases decreases with temperature. In order to make the appropriate fit it was necessary to use Benson's restricted rotor approach. The basic

TABLE 1: Calculated Thermochemistries, Energies, Zero Point Energies, and BAC's for Stable Molecules

		thermochemistry		symmetry	E_{MP4}^c	E_{zp}^d	E_{spin}^e	E_{BAC}^f	G2; ^g H_f^{298}	exp
species	H_{f298}^a	theory level ^b								
1	SiH ₄	33.8	1	T_{4d}	-291.421 96	0.033 381	0	33.27		
2	SiH ₂	277.9	1	C_{2v}	-290.157 07	0.012 657	0	15.55		
3	SiO	-101.9	1	C_{infv}	-364.191 11	0.003 205	0	18.27	-94.4	-101.2
4	HSiO	28.8	1	C_s	-364.722 56	0.009 521	4.01	25.67	35.5	
5	SiOH	-1.6	1	C_s	-364.733 12	0.134 431	3.64	39.33	0.4	
6	H ₂ SiO	-98.2	1	C_{2v}	-365.358 87	0.020 361	0	34.82	-98.2	
7	HSiOH (trans)	-91.0	1	C_s	-365.353 78	0.022 489	0	59.52		
8	H ₃ SiOH	-281.7	1	C_s	-366.596 97	0.041 314	0	64.79	-282.1	
9	H ₂ SiOH	-109.1	1	C_s	-365.944 52	0.030 411	0.84	56.05	-107.0	
10	H ₃ SiO	16.7	1	C_s	-365.901 71	0.029 577	3.05	36.24	4.1	
11	SiO ₂	-288	1	D_{infh}	-439.318 18	0.007 684	0	36.95	-276.7	-310.6
12	HSiO ₂	-155.9	1	C_s	-439.852 54	0.015 323	3.38	39.12	-157.5	
13	HOSiO	-313.5	1	C_s	-439.908 47	0.010 805	3.18	58.44	-304.7	
14	HSiO(OH)	-471.1	1	C_s	-440.555 23	0.028 347	0	36.21	-462.3	
15	Si(OH) ₂	-492.4	1	C_{2v}	-440.561 23	0.030 261	0	67.46	-491.1	
16	HSi(OH) ₃	-995.0	1	C_s	-516.976 63	0.055 162	0	128.3		
17	Si ₂ O ₂ cyc	-414.2	2	C_{2v}	-728.191 38	0.009 388	0	172.63		-405.5
18	Si ₃ O ₃ cyc	-743.6	2	C_{3v}	-1092.337 60	0.015 251	0	276.88		
19	Si ₄ O ₄ cyc	-1004.4	2	C_{4v}	-1456.450 20	0.019 678	0	380.21		
20	Si ₂ O ₂ H(OH) cyc	-929.6	2	C_s	-804.514 66	0.035 498	0	294.73		
21	Si ₃ O ₃ H(OH) cyc	-1263	2	C_s	-1168.664 20	0.041 051	0	397.01		
22	(HSiO(OH)) ₂	-1402.3	2	C_s	-880.831 01	0.061 158	0	414.24		
23	(H ₂ SiO) ₂	-657.9	2	C_{2v}	-730.611 11	0.048 194	0	262.75		
24	(HSiO) ₂	-538.3	2	C_{2v}	-729.405 51	0.028 852	0	217.41		

^a H_f^{298} = enthalpy of formation at 298 K (kJ/mol). ^b Theory level: 1, BAC-MP4 calculated at MP4/6-311G(2DF,P)//MP2/6-31G(D); 2, BAC-MP4 calculated at MP4/6-31G(D,P)//HF/6-31G(D). ^c E_{MP4} = MP4 energy in hartrees. ^d E_{zp} = zero point energy in hartrees. ^e E_{spin} = spin correction kJ/mol. ^f E_{BAC} = bond additivity correction in kJ/mol. ^g G2 calculations by: Darling, C. L.; Schlegel, H. B. *J. Phys. Chem.* **1993**, *97*, 8207.

TABLE 2: HF/6-31G* Vibrational Frequencies (cm⁻¹; Scaled by 0.89) for Equilibrium Stable Molecules

SiH ₄	910.1, 910.1, 910.1, 940.7, 940.7, 2115.9, 2115.9, 2115.9, 2123.2
SiH ₂	1009.4, 1970.7, 1980.5
SiO	1256.1
HSiO	677.4, 1160.8, 1892.7
SiOH	790.2, 820.2, 3658.0
H ₂ SiO	700.7, 722.4, 1003.7, 1210.0, 2171.6, 2172.2
HSiOH (trans)	623.2, 780.1, 825.3, 937.7, 1966.3, 3681.4
H ₃ SiOH	180.5, 657.5, 708.0, 815.8, 855.4, 929.1, 953.8, 988.3, 2110.7, 2125.0, 2165.1, 3702.7
H ₂ SiOH	933.3, 2085.6, 2093.2, 3675.9
H ₃ SiO	688.6, 795.2, 795.6, 920.2, 965.9, 967.5, 2149.1, 2153.3, 2156.5
SiO ₂	293.7, 293.7, 992.0, 1431.9
HSiO ₂	318.8, 569.1, 781.2, 859.0, 1248.7, 2228.5
HOSiO (trans)	311.7, 315.8, 759.8, 818.6, 1184.7, 3681.9
HSiO(OH)	329.8, 454.2, 600.2, 790.5, 877.3, 897.0, 1243.8, 2242.7, 3674.3
Si(OH) ₂	312.3, 444.1, 497.1, 775.6, 786.6, 833.5, 879.8, 3643.5, 3687.2
HSi(OH) ₃	148.4, 200.5, 228.8, 301.0, 348.7, 387.6, 744.8, 766.7, 806.6, 814.7, 827.9, 879.0, 933.4, 947.1, 2199.8, 3688.5, 3695.0, 3700.3
Si ₂ O ₂	255.1, 518.5, 541.9, 742.4, 783.6, 837.7
Si ₃ O ₃	117.1, 117.2, 217.9, 305.3, 305.3, 540.7, 571.3, 599.6, 599.6, 723.5, 940.2, 940.4
Si ₄ O ₄	-39.1, 28.6, 88.9, 109.2, 109.2, 169.8, 200.4, 333.5, 333.8, 396.4, 531.0, 531.0, 558.1, 562.4, 776.9, 985.3, 985.3, 1012.3
Si ₂ O ₂ H(OH)	156.2, 170.9, 319.4, 386.7, 535.5, 586.0, 724.6, 768.9, 798.7, 836.7, 858.9, 874.9, 940.8, 2259.7, 3694.5
Si ₃ O ₃ H(OH)	69.0, 84.6, 117.1, 177.2, 272.9, 278.0, 316.2, 384.2, 526.1, 574.5, 599.1, 627.2, 767.5, 775.1, 865.5, 880.5, 899.4, 963.1, 975.9, 2234.5, 3701.9
(HSiO(OH)) ₂ silinoic acid dimer	112.4, 126.7, 158.7, 270.9, 300.0, 350.4, 436.2, 519.6, 629.2, 692.9, 756.3, 771.3, 782.2, 817.5, 825.6, 870.3, 885.3, 915.8, 925.1, 959.5, 2235.4, 2238.8, 3694.2, 3694.7
(H ₂ SiO) ₂ silanone dimer	218.5, 541.4, 594.0, 605.6, 628.5, 656.3, 712.8, 728.1, 812.1, 844.1, 855.2, 974.3, 979.8, 1010.6, 2175.9, 2178.9, 2180.9, 2191.3
(HSiO) ₂	255.1, 540.6, 572.5, 601.2, 697.5, 729.2, 793.5, 841.2, 917.9, 993.3, 2180.6, 2185.0

procedure has been successfully employed to model hydrocarbon decomposition reactions, and the assumption, probably justified, is that the general procedures can be carried over to silicon systems.

Results and Discussion

Previous experimental results on high-temperature combustion of silane to yield fine particles have suggested that water vapor plays an important role in the catalysis of the oxidation and

that under diffusion flame conditions, where little oxygen is available to initiate attack, the pyrolysis of silane to silylene must initiate the chemistry. Figure 1 outlines the reactions studied in this work. In large part the pathways chosen for study were determined by comparison with in-situ gas phase species measurements made in a nanophase Si/SiO₂ particle-forming reactor in conjunction with detailed chemical kinetic modeling.^{10,18-21} Tables 1-7 contain a summary of the thermodynamic and kinetic information that has been derived during the course of this work. In subsequent sections we will highlight some of the key aspects of these results.

TABLE 3: HF/6-31G* Moments of Inertia (au) for Equilibrium Stable Molecules

SiH ₄	85.39	85.39	85.39
SiH ₂	243.74	208.25	112.3
SiO	0.00	86.44	86.44
HSiO	5.32	94.21	99.53
SiOH	2.50	109.96	112.46
H ₂ SiO	10.81	100.17	110.99
HSiOH (trans)	10.39	112.53	122.92
H ₃ SiOH	23.43	133.18	135.91
H ₂ SiOH	16.12	123.02	132.12
H ₃ SiO	21.20	127.42	127.52
SiO	0.00	267.97	267.97
HSiO ₂	38.75	235.32	274.07
HOSiO (trans)	26.58	252.20	278.78
HSiO(OH)	43.25	241.21	284.46
Si(OH) ₂	70.56	203.60	274.25
HSi(OH) ₃	252.18	283.26	462.08
Si ₂ O ₂	149.64	309.15	458.80
Si ₃ O ₃	671.38	671.43	1342.82
Si ₄ O ₄	1452.36	1453.02	2905.39
Si ₂ O ₂ H(OH)	210.17	649.43	742.19
Si ₃ O ₃ H(OH)	746.91	1175.23	1797.12
(HSiO(OH)) ₂ silinoic acid dimer	246.94	1117.68	1177.34
(H ₂ SiO) ₂ silanone dimer	176.32	366.36	500.83
(HSiO) ₂	162.86	338.49	480.42

Reactions of SiH₂ + H₂O. On the basis of the previous experimental and numerical results,^{3,18-21} we had concluded that oxidation of silicon species was taking place in an anaerobic environment but in the presence of a substantial concentration of water vapor. Since it is well-known that the primary product of silane pyrolysis is singlet silylene (SiH₂), we had proposed that this species must be directly involved in oxidation. Figure 2 contains a potential energy diagram describing the interaction of silylene with water and the subsequent consequences. Hot silanol (with a computed heat of formation of -281.7 kJ/mol) from insertion is the initial product. The initial complex forms through an overlap of the lone pair in oxygen into the empty p orbital in Si (as an out-of-plane bent structure) and is stabilized

in a 29 kJ/mol well with a long Si-O bond length of 2 Å. The transition state to silanol (H₃SiOH) was found to require 10.4 kJ/mol activation and involves a 1,2 hydrogen shift. Raghavachari et al.²² have also calculated this reaction and showed it to require a somewhat higher barrier of 38 kJ/mol.

In comparison, singlet methylene insertion into water has no activation energy to form methanol. Formaldehyde lies 83 kJ/mol above methanol, in comparison to 184 kJ/mol for the silicon analog.

We have found two low-lying channels for the decomposition of silanol. They involve 1,1 and 1,2 hydrogen shifts leading to the production of H₂SiO and HSiOH with heats of formation of -98.2 and -91.7 kJ/mol, respectively. Two endothermic decomposition reactions, involving hydrogen atom ejection, have also been considered. Solution of the kinetic relations shows that the most endothermic process, involving the formation of the H₃SiO radical, does not make any contribution. However, at the highest temperatures, the ejection of the hydrogen atom from the silicon atom is as important as the two H₂ ejection channels. This is a reflection of the larger A-factors for the hydrogen atom ejection overcoming the activation energy deficit. At the lowest temperatures and increasingly higher pressures, stabilization is of some importance. In the intermediate temperature range (from 600 K up) the two H₂-producing channels are predominant and continue to be the key processes until overtaken at the highest temperatures by the hydrogen atom ejection reaction. These effects also have a pressure component, since, as the pressure is increased, the lower energy decomposition channels are increasingly favored. There is thus a whole spectrum of reactivity as one scans the temperature and pressure ranges. The kinetic results are summarized in Figure 3 for rate constants at 1 atm.

Reactions of H₃SiOH. While silanone and its isomer HSiOH are the predominant products from silylene and H₂O at moderate to higher temperatures, higher pressures (as might be found in application for scramjet ignition) might show significant

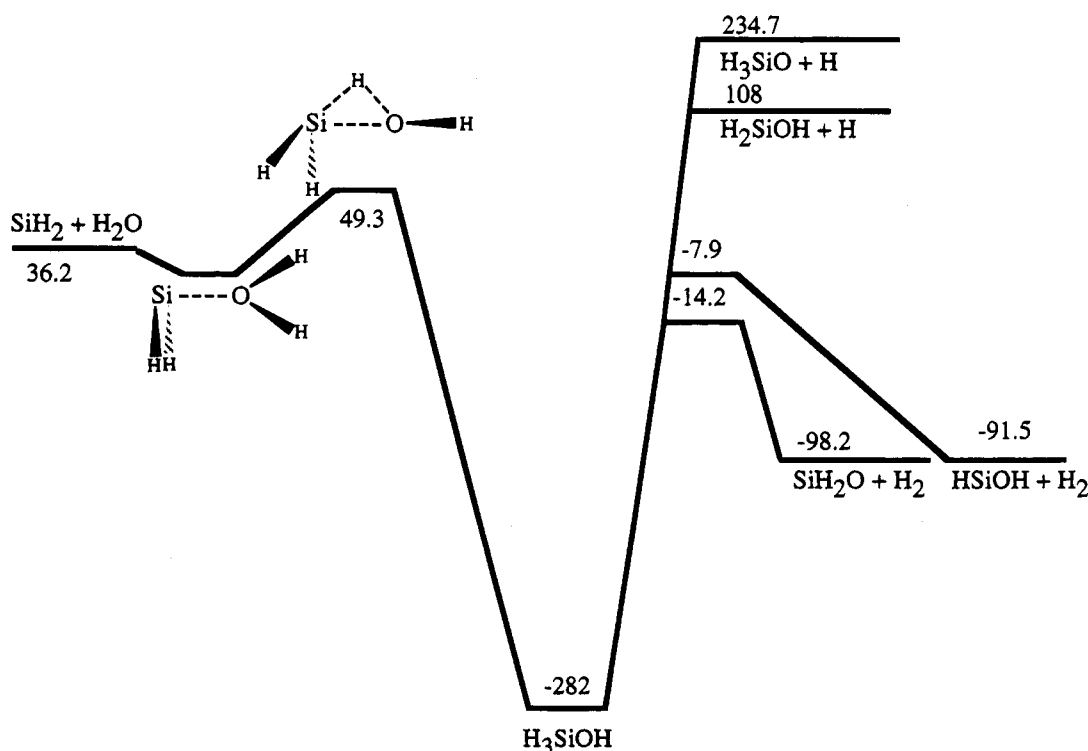
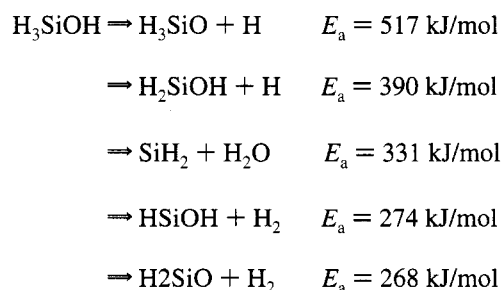
**Figure 2.** Energy diagram for SiH₂ + H₂O.

TABLE 4: Calculated Thermochemistries, Energies, Zero Point Energies, and BAC's for Transition States

	reaction	H_f^{298} ^a	E_a ^b	theory level ^c	E_{MP4} ^d	E_{zp} ^e	E_{spin} ^f	E_{BAC} ^g
1	SiH ₂ + H ₂ O → H ₃ SiOH	49.3	10.5	1	-366.464 98	0.037 195	0	68.76
2	H ₃ SiOH → H ₂ SiO + H ₂	-14.2	268.4	1	-366.389 26	0.036 331	0	65.04
3	H ₂ SiO + H ₂ O → HSiO(OH) + H ₂	-328.1	12.5	1	-441.663 85	0.044 417	0	96.14
4	HSiO(OH) → SiO + H ₂ O	-191.1	280.1	1	-440.442 54	0.023 091	0	69.81
5	HSiO(OH) → Si(OH) ₂	-256.7	214.4	1	-440.467 61	0.023 246	0	70.64
6	HOSiO → SiO + OH	-71.5	250.4	1	-439.817 54	0.014 311	3.97	45.48
7	HOSiO (cis) → HOSiO (trans)	-304.7	8.8	1	-439.903 61	0.016 883	3.32	57.89
8	HOSiO → HSiO ₂	-122.5	191.1	1	-439.830 31	0.011 361	7.41	49.78
9	HOSiO → SiO ₂ + H	-59.4	254.1	1	-439.802 92	0.007 582	10.49	47.07
10	H ₃ SiOH → HSiOH + H ₂	-7.9	273.8	1	-366.486 74	0.037 051	0	68.68
11	H ₂ SiO → SiO + H ₂	234.1	332.3	1	-365.226 75	0.014 561	0	35.57
12	HSiO → SiOH	142.1	113.3	1	-364.670 84	0.006 588	11.04	33.31
13	SiOH → SiO + H	166.4	168.1	1	-364.655 25	0.003 754	23.78	30.31
14	HSiO → SiO + H	98.2	79.4	1	-364.690 21	0.003 607	10.78	20.31
15	HSiOH → H ₂ SiO	129.6	221.1	1	-365.266 11	0.015 401	0	38.41
16	HSiOH → SiO + H ₂	64.1	155.5	1	-365.287 67	0.015 891	0	47.57
17	H ₂ SiOH → H ₂ SiO + H	134.6	245.8	1	-365.836 81	0.020 001	22.95	45.73
18	H ₂ SiOH → HSiO + H ₂	132.1	241.2	1	-365.845 58	0.025 262	3.64	55.84
19	H ₃ SiOH → H ₂ SiO + H	99.1	82.3	1	-365.855 72	0.020 815	17.47	39.38
20	H ₃ SiO → HSiO + H ₂	132.1	115.4	1	-365.845 57	0.025 731	3.64	55.76
21	H ₂ SiO + H → HSiO + H ₂	120.8	1.3	1	-365.848 95	0.019 218	7.02	41.26
22	H ₃ SiO → H ₂ SiOH	78.6	60.2	1	-365.866 71	0.024 991	8.82	48.45
23	Si ₂ O ₂ + H ₂ O → Si ₂ O ₂ H(OH)	-589.4	67.3	2	-804.382 98	0.031 019	0	289.09
24	Si ₃ O ₃ + H ₂ O → Si ₃ O ₃ H(OH)	-917.5	68.6	2	-1168.531 10	0.037 157	0	389.71
25	HSiO(OH) → SiO ₂ + H ₂	-229.4	241.6	1	-440.456 84	0.022 336	0	67.97
26	Si(OH) ₂ → SiO + H ₂ O	-336.5	155.8	1	-440.496 15	0.025 841	0	81.01
27	Si(OH) ₂ + H ₂ O → HSi(OH) ₃	-655.8	105.4	1	-516.842 25	0.051 351	0	130.8
28	H + H ₃ SiOH → H ₂ SiOH + H ₂	-51.4	12.5	1	-367.082 88	0.040 583	5.68	72.41
29	H + H ₃ SiOH → H ₃ SiO + H ₂	13.4	84.7	1	-367.057 31	0.038 137	8.86	64.96
30	H + HSiOH → SiOH + H ₂	112.9	0	1	-365.849 11	0.021 159	8.86	52.79
31	H + HSiOH → HSiO + H ₂	175.6	50.2	1	-365.822 58	0.018 482	10.83	49.45
32	H + HSiO(OH) → HOSiO + H ₂	-246.6	2.09	1	-441.043 53	0.027 207	6.56	73.92
33	(H ₂ SiO) ₂ → (HSiO) ₂ + H ₂	305.7	351.9	2	-730.472 63	0.042 536	0	259.49
Reactions with No Defined Transition State								
34	Si ₂ O ₂ → SiO + SiO		210.3	2				
35	Si ₃ O ₃ → Si ₂ O ₂ + SiO		227.4	2				
36	Si ₄ O ₄ → Si ₃ O ₃ + SiO		158.8	2				
37	HSiOH → SiOH + H		303.5	1				
38	(H ₂ SiO) ₂ → 2 H ₂ SiO		473.2	2				
39	(HSiO(OH)) ₂ → 2 HSiO(OH)		473.6	2				
40	H + HSiO → SiO + H ₂		0	1				
41	OH + H ₃ SiOH → H ₂ SiO + H ₂ O		0	1				
42	OH + HSiOH → HSiO + H ₂ O		0	1				

^a H_f^{298} = enthalpy of formation at 298 K (kJ/mol). ^b E_a = activation energy (kJ/mol). ^c Theory level: 1, BAC-MP4 calculated at MP4/6-311G(2DF,P)//MP2/6-31G(D); 2, BAC-MP4 calculated at MP4/6-31G(D,P)//HF/6-31G(D). ^d E_{MP4} = MP4 energy hartrees. ^e E_{zp} = zero point energy (hartrees). ^f E_{spin} = spin correction (kJ/mol). ^g E_{BAC} = bond additivity correction (kJ/mol).

stabilization of this species. Unimolecular decomposition of silanol can proceed through five channels, as seen in Figure 2.



The lowest energy paths are effectively evenly divided between HSiOH and H₂SiO, with the formation of silylene less important, in agreement with the calculations of Gordon and Pederson.²³ The RRKM/master equation treatment for silanol can be applied in an analogous manner to the decomposition of hot silanol. As can be seen from Figure 5, all reactions are in the pressure dependent region. As in the case for the hot silanol, the preferred channels are the decomposition to silanone and its isomer. The SiH₂ + H₂O formation channel is

particularly retarded due to the depletion of the tail of the silanol distribution function by the lower lying decomposition pathways.

The energetic ordering of the various unimolecular decomposition channels of silanol is similar to that calculated for methanol decomposition.²⁴ The O—H bond strength in silanol is comparable to that in methanol. However ejection of H from the silicon center is favored over that from the carbon due to a lower bond strength of the Si—H bond. The heats of formation and activation barriers for the 1,1 and 1,2 decomposition of silanol are essentially equivalent. This is in contrast to methanol which has similar activation barriers for these two channels, but H₂CO is more than 200 kJ/mol more stable, implying that in a relative thermodynamic sense the C=O bond is considerably stronger than the Si=O bond. This is consistent with the general feature of Si as a poor π bonding element.

Due to the significant activation energy for these processes, reactions of silanol with reactive radicals such as OH and H atoms must be considered. Transition states determined from our calculations show that the low-energy pathway for reaction involves abstraction of the Si—H bond. The activation energies have been found to be 12 kJ/mol and zero for H and OH, respectively, while H atom abstraction from the O—H bond

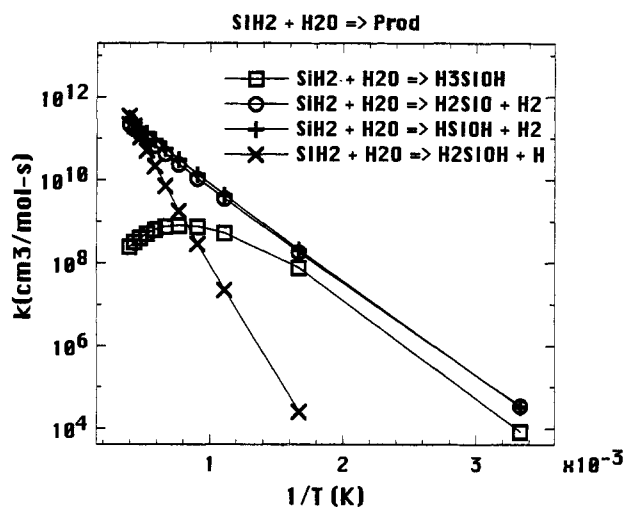
TABLE 5: HF/6-31G* Vibrational Frequencies (Scaled by 0.89) for Transition States

SiH ₂ + H ₂ O → H ₃ SiOH	-1898.5, 371.7, 516.2, 566.3, 731.9, 825.3, 957.0, 1029.2, 1792.9, 2078.1, 2103.8, 3604.8
H ₃ SiOH → H ₂ SiO + H ₂	-1768.6, 549.2, 681.0, 784.5, 905.0, 989.5, 1105.9, 1181.8, 1778.0, 1915.5, 2171.2, 2178.0
HSiOOH → SiO + H ₂ O	-1883.3, 256.8, 359.5, 472.9, 627.9, 886.8, 1217.3, 1727.6, 3501.6
HSiOOH →: Si(OH) ₂	-1673.8, 190.0, 307.8, 367.0, 727.8, 847.7, 1115.9, 1927.7, 3626.9
H ₂ SiO + H ₂ O → HSiOOH + H ₂	-1847.2, 272.8, 465.0, 613.2, 662.0, 774.0, 785.3, 908.4, 1040.4, 1204.1, 1364.4, 1671.3, 1827.8, 2217.7, 3601.6
HOSiO (cis) → HOSiO (trans)	-358.7, 326.5, 598.8, 821.1, 1189.4, 3680.9
HOSiO → HSiO ₂	-1957.7, 286.6, 332.0, 803.9, 1256.9, 1773.4
H + SiO ₂ → HOSiO	-1563.1, 210.4, 302.6, 332.8, 831.4, 1294.5
OH + SiO → HOSiO	-204.6, 124.4, 130.0, 548.6, 1244.9, 3560.8
H ₃ SiOH → HSiOH + H ₂	-1544.9, 321.9, 566.5, 702.2, 757.6, 810.8, 928.5, 1040.3, 1484.3, 2037.5, 2169.8, 3699.8
H ₂ SiO → H ₂ + SiO	-2145.6, 585.9, 624.4, 1136.5, 1279.5, 2094.7
HSiO → SiOH	-2164.5, 870.9, 1710.9
SiOH → SiO + H	-2209.9, 556.5, 914.8
HSiO → SiO + H	-525.3, 174.3, 1239.1, -1868.2, 272.9, 773.7, 1056.8, 1908.8, 2024.2
HSiOH (cis) → SiO + H ₂	-2272.6, 686.3, 1064.3, 1142.7, 1531.7, 1802.2
H ₂ SiOH → H ₂ SiO + H	-846.9, 280.5, 315.1, 435.6, 664.9, 866.6, 945.3, 2162.9, 2175.6
H ₂ SiOH → HSiO + H ₂	-1969.7, 634.1, 679.8, 814.3, 1002.9, 1129.7, 1721.7, 1873.2, 2045.2
H ₃ SiO → H ₂ SiO + H	-548.4, 164.3, 293.2, 680.1, 707.6, 985.8, 1066.2, 2128.5, 2132.2
H ₂ SiO → HSiO + H ₂	-1885.9, 495.0, 719.5, 955.0, 1047.0, 1219.5, 1708.6, 1910.8, 2029.2
H + H ₂ SiO → HSiO + H ₂	-1927.1, 222.7, 332.9, 747.1, 916.3, 974.5, 1048.5, 1208.2, 2081.9
H ₂ SiO → H ₂ SiOH	-2131.3, 599.5, 644.1, 707.8, 827.6, 953.3, 1758.1, 2148.1, 2156.2
HSiOOH → SiO ₂ + H ₂	-1703.9, 299.8, 371.5, 883.6, 991.7, 1091.1, 1391.8, 1795.3, 1929.0
:Si(OH) ₂ → SiO + H ₂ O	-1638.5, 415.6, 451.6, 680.1, 693.5, 1062.6, 1283.4, 1888.9, 3651.9
:Si(OH) ₂ + H ₂ O → HSi(OH) ₃	-1825.6, 175.9, 255.2, 292.9, 327.4, 351.6, 403.4, 560.3, 687.4, 786.3, 802.5, 861.2, 892.5, 1038.0, 1777.9, 3563.9, 3654.4, 3695.5
H + H ₃ SiOH → H ₂ + H ₂ SiOH	-1811.5, 180.7, 306.6, 478.1, 705.7, 756.8, 822.1, 937.0, 942.7, 1022.8, 1030.9, 1052.7, 2102.9, 2103.6, 3462.5
H + H ₃ SiOH → H ₂ + H ₂ SiO	-2804.1, 138.4, 312.4, 670.9, 674.8, 744.7, 773.0, 897.4, 919.9, 943.1, 971.1, 1455.7, 2138.0, 2146.2, 2161.1
H + HSiOH → H ₂ + SiOH	-1632.0, 152.4, 211.1, 711.5, 799.6, 827.0, 908.9, 1007.8, 3674.0
H + HSiOH → H ₂ + HSiO	-3068.7, 255.2, 349.3, 767.5, 773.1, 795.4, 961.2, 1402.0, 1969.9
H + HSiOOH → SiOOH + H ₂	-1943.6, 203.5, 212.7, 316.3, 437.0, 794.9, 857.8, 920.1, 994.0, 1043.5, 1236.1, 3646.8
Si ₂ O ₂ + H ₂ O → Si ₂ O ₂ H(OH)	-1843.6, 146.6, 185.1, 324.6, 363.5, 556.4, 584.9, 600.4, 672.0, 775.4, 796.4, 845.7, 987.2, 1766.0, 3552.4
Si ₃ O ₃ + H ₂ O → Si ₃ O ₃ H(OH)	-1830.3, 59.9, 100.9, 169.0, 206.2, 269.9, 307.8, 340.5, 466.5, 543.3, 570.6, 573.8, 599.6, 629.4, 766.8, 776.0, 949.4, 955.9, 1046.4, 1782.3, 3448.4
(H ₂ SiO) ₂ → (HSiO) ₂ + H ₂	-1757.8, 206.3, 466.2, 528.6, 602.2, 644.2, 650.9, 707.4, 735.5, 792.8, 835.0, 847.0, 935.6, 986.6, 1235.9, 2120.1, 2184.7, 2191.8

TABLE 6: HF/6-31G* Moments of Inertia (au) for Transition States

SiH ₂ + H ₂ O → H ₃ SiOH	21.71	163.96	167.78
H ₃ SiOH → H ₂ SiO + H ₂	27.50	117.39	123.81
HSiOOH → SiO + H ₂ O	46.41	264.74	306.83
HSiOOH →: Si(OH) ₂	42.57	249.32	288.79
H ₂ SiO + H ₂ O → HSiOOH + H ₂	71.89	267.44	311.57
HOSiO (cis) → HOSiO (trans)	27.38	255.96	278.69
HOSiO → HSiO ₂	11.00	270.58	281.58
H + SiO ₂ → HOSiO	0.00	300.85	300.85
OH + SiO → HOSiO	52.19	504.99	557.18
H ₃ SiOH → HSiOH + H ₂	24.46	135.43	139.15
H ₂ SiO → H ₂ + SiO	10.01	106.60	116.61
HSiO → SiOH	5.42	93.94	99.36
SiOH → SiO + H	3.31	98.83	102.14
HSiO → SiO + H	12.88	95.59	108.47
HSiOH → H ₂ SiO	11.56	103.25	114.81
HSiOH (cis) → SiO + H ₂	16.01	96.91	112.93
H ₂ SiOH → H ₂ SiO + H	14.49	117.42	124.23
H ₂ SiOH → HSiO + H ₂	21.60	107.13	118.51
H ₃ SiO → H ₂ SiO + H	23.18	108.17	110.28
H ₂ SiO → HSiO + H ₂	21.60	107.18	118.56
H + H ₂ SiO → HSiO + H ₂	25.48	120.55	146.03
H ₃ SiO → H ₂ SiOH	16.89	116.18	120.68
HSiOOH → SiO ₂ + H ₂	21.41	270.58	291.99
:Si(OH) ₂ → SiO + H ₂ O	95.64	175.44	267.41
:Si(OH) ₂ + H ₂ O → HSi(OH) ₃	256.76	314.94	488.48
H + H ₃ SiOH → H ₂ + H ₂ SiOH	46.83	142.78	168.63
H + H ₃ SiOH → H ₂ + H ₃ SiO	38.41	148.72	166.22
H + HSiOH → H ₂ + SiOH	37.17	115.33	152.50
H + HSiOH → H ₂ + HSiO	22.56	125.76	148.32
H + HSiOOH → SiOOH + H ₂	77.02	244.29	321.32
Si ₂ O ₂ + H ₂ O → Si ₂ O ₂ H(OH)	232.93	659.74	736.63
Si ₃ O ₃ + H ₂ O → Si ₃ O ₃ H(OH)	792.45	1165.07	1743.25
(H ₂ SiO) ₂ → (HSiO) ₂ + H ₂	179.67	368.64	501.17

requires 77 kJ/mol to form the H₃SiO radical (Figure 4). OH radical attack on the Si-H bond of silanol to form H₂O + H₂-SiOH proceeds spontaneously without an activation barrier.

Figure 3. Calculated SiH₂ + H₂O rate constants at 1 atm.

Reactions of SiH₂O and HSiOH. Once silanone is formed, it can undergo unimolecular decomposition to SiO + H₂ (thermoneutral), react with H₂O, or undergo abstraction by a radical species. Direct unimolecular decomposition of silanone as calculated by Kudo and Nagase²⁵ (355 kJ/mol) or calculations performed here (332 kJ/mol) proceeds with a large activation barrier and is therefore unlikely to be important (Figure 6). Silanone can also isomerize by a 1,2 hydrogen shift to cis or trans hydroxysilylenes (barrier of 221 kJ/mol) and then subsequently decompose through a lower barrier than the 1,1 route to SiO + H₂ (barrier of 155 kJ/mol). This is in contrast to the results of Tachibana et al.,²⁶ who calculated significantly higher barriers of 267 and 209 kJ/mol for the two reactions, respectively. Even though the net reaction is thermoneutral (also the

TABLE 7: RRKM/Master Equation Derived Rate Constants (mol cm⁻³ s⁻¹) for Selected Reactions^a

reaction	A	n	E _g /R
SiH ₂ + H ₂ O ⇒ H ₃ SiOH	2.80E+31 ^b	-6.37	8.12E+03
SiH ₂ + H ₂ O ⇒ H ₂ SiO + H ₂	3.84E+10	-.61	4.89E+03
SiH ₂ + H ₂ O ⇒ HSiOH + H ₂	2.15E+10	0.73	4.94E+03
SiH ₂ + H ₂ O ⇒ H ₂ SiOH + H	6.10E+06	1.95	1.08E+04
H ₃ SiOH ⇒ H ₂ SiO + H ₂	2.01E+27	-4.3	3.43E+04
H ₃ SiOH ⇒ HSiOH + H ₂	2.20E+26	-4.2	3.35E+04
H ₂ SiO + H ₂ O ⇒ HSiO(OH) + H ₂	3.60E+09	0.43	3.87E+03
HSiO(OH) ⇒ Si(OH) ₂	1.04E+33	-4.7	2.86E+04
OH + SiO ⇒ HOSiO	2.10E+23	-3.6	9.56E+02
OH + SiO ⇒ H + SiO ₂	1.80E+10	0.78	6.13E+02
H + SiO ₂ ⇒ HOSiO	8.50E+24	-4	2.85E+03
HSiO ⇒ SiO + H	2.00E+20	-1.2	1.08E+04
HSiOH ⇒ SiO + H ₂	9.40E+28	-3.8	1.94E+04
H ₂ SiOH ⇒ HSiO + H ₂	9.60E+27	-3.4	3.01E+04
H + H ₂ SiO ⇒ H ₂ SiOH	6.50E+24	-3.6	4.14E+03
H + H ₂ SiO ⇒ HSiO + H ₂	5.40E+11	0.58	3.64E+03
H ₃ SiO ⇒ H ₂ SiOH	1.50E+24	-2.6	7.76E+03
Si ₂ O ₂ + H ₂ O ⇒ Si ₂ O ₂ H(OH)	2.70E+01	3.2	8.26E+03
Si ₃ O ₃ H ₂ O ⇒ Si ₃ O ₃ H(OH)	9.25E+01	3	8.83E+03
Si(OH) ₂ ⇒ SiO + H ₂ O	1.50E+31	-4.4	2.10E+04
H + H ₃ SiOH ⇒ H ₂ SiOH + H ₂	1.74E+08	1.77	7.20E+02
H + H ₃ SiOH ⇒ H ₃ SiO + H ₂	2.20E+07	1.89	4.47E+03
H + H ₂ SiOH ⇒ H ₂ SiO + H ₂	3.31E+20	-2.04	1.78E+03
H + H ₂ SiOH ⇒ HSiOH + H ₂	6.16E+20	-1.98	1.81E+03
H + H ₂ SiOH ⇒ SiH ₂ + H ₂ O	2.24E+15	-0.65	2.11E+03
H + H ₃ SiO ⇒ H ₂ SiO + H ₂	1.58E+18	-1.37	7.05E+02
H + H ₃ SiO ⇒ H ₂ + HSiOH	1.63E+18	-1.33	6.85E+02
H + H ₃ SiO ⇒ SiH ₂ + H ₂ O	9.56E+13	-0.34	2.50E+02
H + H ₃ SiO ⇒ H ₃ SiOH	1.23E+12	0.52	7.80E+01
H + HSiO(OH) ⇒ HOSiO + H ₂	9.86E+07	1.83	7.62E+02
Si ₂ O ₂ ⇒ SiO + SiO	1.30E+34	-6.56	2.77E+04
Si ₃ O ₃ ⇒ Si ₂ O ₂ + SiO	2.70E+51	-11.3	3.25E+04
Si ₄ O ₄ ⇒ Si ₃ O ₃ + SiO	3.22E+42	-8.9	2.30E+04
(H ₂ SiO) ₂ ⇒ 2H ₂ SiO	3.60E+38	-6.8	5.65E+03
2H ₂ SiO ⇒ (HSiO) ₂ + H ₂	2.00E+23	-3.1	5.60E+03
(HSiO(OH)) ₂ ⇒ 2HSiO(OH)	1.70E+49	-9.6	6.19E+03

^a All rate constants are at 1 atm. ^b Read as 2.80 × 10³¹.

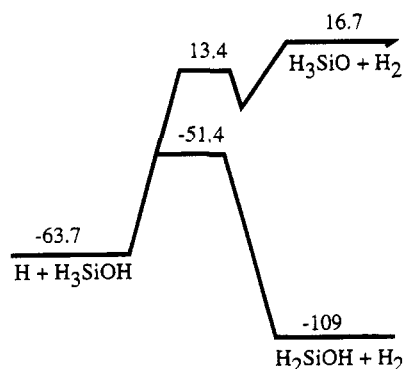


Figure 4. Energy diagram for H + H₃SiOH.

case for the carbon analog), silanone should be relatively stable to decomposition. In the presence of water vapor, however, the reaction should proceed quite fast, as shown by the potential energy profiles illustrated in Figure 7. As in the silylene-water reactions, H₂O complexes with the silicon atom on silanone at about 2 Å, after which one can proceed without a barrier to silanediol (H₂Si(OH)₂; H_f²⁹⁸ = -637 kJ/mol) (as previously shown by Kudo and Nagase²⁷) or alternatively through a 12.5 kJ/mol barrier to the silicon analog of formic acid (silanoic acid, HSiO(OH); H_f²⁹⁸ = -471 kJ/mol). In turn silanoic acid can undergo rapid abstraction of H by OH or O to yield HOSiO.

Silanone energetics for abstraction reactions with H or OH to the corresponding formyl radical is shown in Figure 8. The barrier to abstraction by the H atom is effectively zero (1.2 kJ/mol). The corresponding reaction with OH showed no saddle

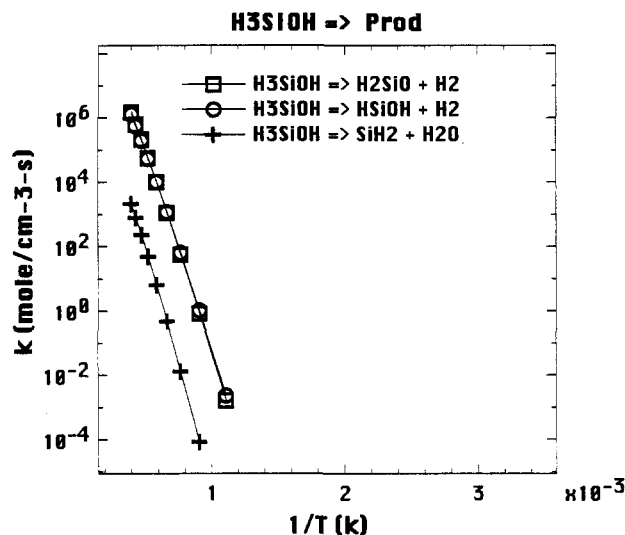


Figure 5. RRKM calculation of H₃SiOH decomposition rate constants at 1 atm.

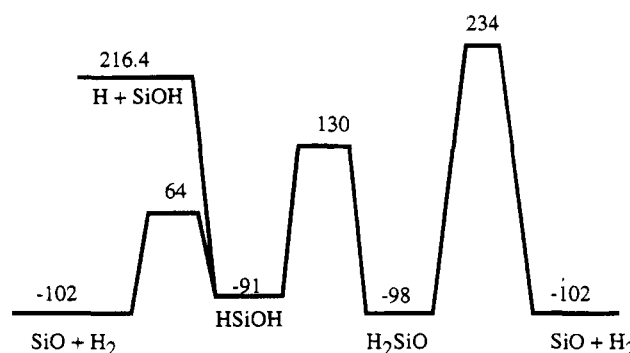


Figure 6. Energy diagram for H₂SiO decomposition.

point for the abstraction to H₂O. The H atom can also insert into the Si=O double bond (15 kJ/mol barrier) to form the silanol radical, which can isomerize to H₃SiO.

In keeping with the bond strengths, abstraction of the hydrogen H-SiOH by hydrogen requires no activation energy, while the reaction with H-OSiH requires a 50 kJ/mol activation barrier. This potential energy diagram can be seen in Figure 9. The barrier for isomerization of HSiO (H_f²⁹⁸ = -28.9 kJ/mol) ⇒ SiOH (H_f²⁹⁸ = -1.7 kJ/mol) was found to be 142 kJ/mol. This is in agreement with the results of Schaefer and Frenking,²⁸ who calculated a barrier of 153 kJ/mol. However they calculate SiOH to be 46 kJ/mol more stable than HSiO, where we see 29 kJ/mol and G2 calculations give 35 kJ/mol.

Reactions of HSiO(OH). The various unimolecular pathways for silanoic acid decomposition can be found in Figure 7. They involve direct formation of SiO₂ + H₂ and SiO + H₂O and isomerization to the silylene diol followed by decomposition to SiO + H₂O. Multichannel RRKM calculation showed that isomerization is the principal decomposition channel. At sufficiently low pressure SiO + H₂O can be formed directly through a chemically activated route. At higher pressures or lower temperatures the silylene diol will be stabilized and its unimolecular decomposition must be considered.

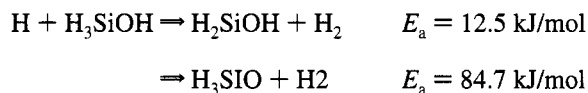
Reactions Involving HOSiO. Formation of silanoic acid (HSiO(OH)) from SiH₂O + H₂O can subsequently proceed, in the presence of a radical pool of H or OH, via abstraction reactions to give HOSiO. Unimolecular decomposition as shown in Figure 10 can lead to either SiO₂ + H or alternatively the more favored channel SiO + OH. SiO₂ and SiO are connected by a chemically activated, essentially thermoneutral water-gas shift reaction.



The chemically activated step shows a pressure dependence below 1000 K and pressures above 0.1 atm when stabilization of HOSiO contributes. The kinetics for formation of HOSiO from either SiO_2 or SiO is shown as a two-channel reaction in which the chemically activated reaction and the stabilization product can form. Reaction of $\text{OH} + \text{SiO}$ requires no barrier and shows the typical pressure dependence found in such reactions. Even at 10 atm the reaction is still not at the high-pressure limit. The reverse reaction of $\text{H} + \text{SiO}_2$ does require a 17 kJ/mol barrier, which makes it considerably slower than the forward reaction. HOSiO can also isomerize to HSiO_2 via a 191 kJ/mol barrier. The carbon analog of course favors the formation of CO_2 over CO , which is perhaps an explanation why SiO_2 is never observed in the gas phase.

Reactions of $\text{Si}_1\text{-O}_1\text{-H}_1$. The energetics of $\text{Si}_1\text{-O}_1\text{-H}_1$ is shown in Figure 11. The presence of H atoms will induce reactions with SiO . As might be expected insertion to the Si atom is more facile and requires no barrier to form HSiO. The less favored route is through attachment to oxygen to form the more stable SiOH. Isomerization between the two will be slow on the basis of the activation barrier, and one should see HSiO as the primary channel. This is an important intermediate, since the reaction of H atoms with silanone to form HSiO is very fast. Darling and Schlegel⁹ have also calculated the barrier to isomerization using G2, in good agreement with our calculations.

Reactions Involving Other $\text{Si}_x\text{O}_y\text{H}_z$ Radicals. Because of the relative weakness of the Si-H bond, radical fragments of stable species should in a relative sense be quite stable. Under specific conditions one might expect to see significant quantities of H_3SiO ($H_f^{298} = 4$ kJ/mol) and H_2SiOH ($H_f^{298} = -26$ kJ/mol), both of which are radicals of the parent silanol. H atom attack on silanol will primarily lead to H_2SiOH (Figure 4).



H_2SiOH can undergo unimolecular decomposition to give $\text{H}_2\text{-SiO}$ (+H) and HSiO (+ H_2), with both having essentially identical barriers of 242 kJ/mol. In contrast, H_3SiO , which has a much higher barrier to its production from silanol, decomposes to H_2SiO (+H) or HSiO (+ H_2) with considerably smaller activation barriers of 105 and 115 kJ/mol, respectively. Isomerization between H_3SiO and H_2SiOH should proceed only in the direction of the formation of H_2SiOH on the basis of energetic considerations (Figure 8). H atom abstraction from methanol to form methoxy (CH_3O) is effectively thermoneutral, although in both the carbon and silicon cases abstraction of H from the silicon or carbon is favored over that of the alcohol H atom.

SiO Clustering. The polymerization of SiO involves successive additions of SiO to form increasingly large rings. The interaction potential for dimer formation as a function of monomer separation distance showed it to be essentially flat till the monomer-monomer separation is decreased to about 2.8 Å, at which point the monomer feels a strong attractive force. This is in qualitative agreement with the Hastie et al.²⁹ matrix isolation experiments, in which the dimer was observed to form at temperatures as low as 5 K.

We have treated the process in the same framework as for radical-radical processes. Rate constants are expected to be close to collisional and are at or near the high-pressure limit at low temperatures. As the temperature is increased, there is a decrease in the rate constants due to the onset of energy transfer

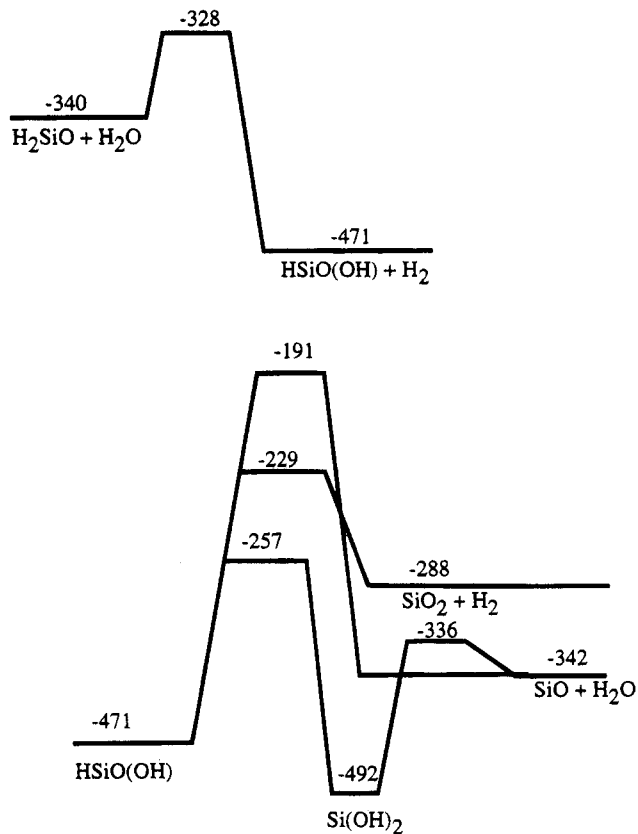


Figure 7. Energy diagram for $\text{H}_2\text{SiO} + \text{H}_2\text{O}$ followed by HSiO(OH) decomposition.

effects. Behaviors for the trimer and tetramer have similar characteristics although the magnitudes of the rate constants are significantly different as are the temperature dependencies. The rate of trimer formation via reaction of monomer with the dimer is 2 orders of magnitude higher than for dimer formation. This behavior is due again to collision efficiency effects and the energetics of the overall reaction. These results demonstrate that the initial state of the condensation process is dependent not only on the concentration of the reactive species but also directly on the pressure of the bath gas or, equivalently, a $(p)^{2+n}$ dependence where n is less than 1. With everything else being equal, the increase in molecular size will lead to a gradual reduction of n .

For the tetramer the rate constant at room temperature is at the high-pressure limit (i.e. pressure independent). This results from a combination of high third body density and the fact that the tetramer has a sufficient number of internal oscillators to dispose of the excess energy more efficiently than the dimer or trimer. As the temperature is increased, the condensation rate constant declines, again due to third body collision effectiveness and to a relatively small density of states for the tetramer (as compared to the trimer with a much deeper well depth). As such, the pressure dependence of the reaction becomes more pronounced as the temperature increases. This is in contrast to the large cluster growth calculated by molecular dynamics methods, which shows a sticking coefficient of 1, resulting from the large number of available oscillators.³⁰

SiO will of course not be the only species capable of clustering. Calculations for the dimerization of silanone and silanoic acid show similar behavior. However, unlike the SiO case, these clusters can undergo both dimerization and chemically activated fragmentation. Interestingly, the dimerization energies for the silanone and silanoic acid are essentially identical and double that of SiO dimerization. The potential

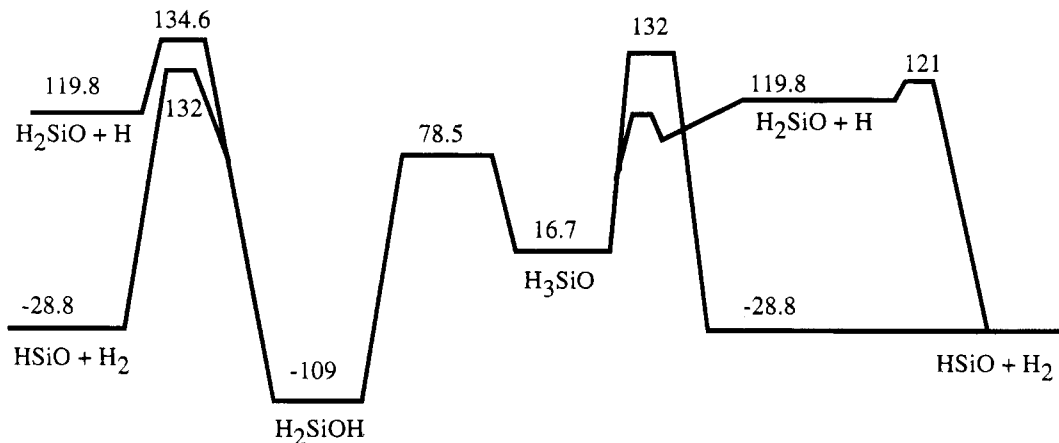


Figure 8. Energy diagram of the shuffle reactions of Si-O-H radicals.

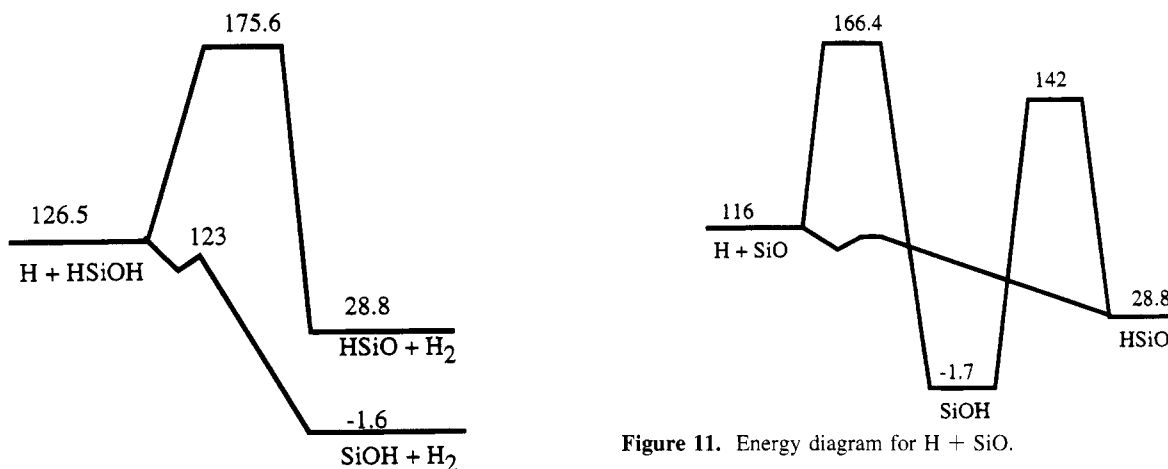


Figure 9. Energy diagram for H + HSioH.

Figure 11. Energy diagram for H + SiO.

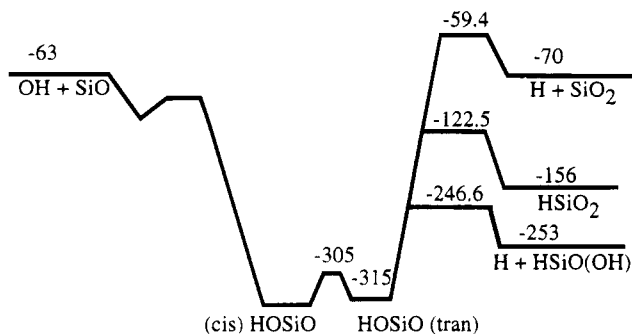


Figure 10. Energy diagram for HOSio decomposition.

energy curves for the two cases are shown below in Figure 13. Kudo and Nagase³¹ have also done calculations on silanone and have shown structures all the way to the tetramer (H_2SiO)₄ while Seidl and Schaefer³² have done an extensive set of calculations on the silanoic acid dimer.

Cluster Oxidation. During the formation of silicon oxides, as with almost all metal oxides, experimental observation has shown that only partial oxidation takes place during the gas phase synthesis process. In many cases, full oxidation requires post-high-temperature oxidation to reach stoichiometric conversion. In many cases high concentrations of water vapor are either present or required, and even under these circumstances oxidation may be incomplete. We investigated cluster oxidation with water vapor by calculating the interaction between H_2O and the dimer and trimer. The initial complex forms through an overlap of the lone pair on oxygen and the empty p orbital on Si (as an out-of-plane bent structure) at a Si-O bond distance

of 2.5 Å. One of the hydrogens on H_2O is stabilized by the adjacent O atom in the dimer. The remaining H atom can then migrate through the transition state to the silicon atom as the Si-O bond distance decreases. The analogous reaction with the trimer proceeds in the same manner. Figure 12 shows the calculated potential energy diagram for the dimer, showing an activation energy of 67 kJ/mol. The trimer has a similar transition state structure with an activation barrier of 69 kJ/mol.

Qualitatively we can see that the reasons for the low oxygen content of metal oxides are that the polymerization of the mono-oxide proceeds without an energy barrier and that the mono-oxide's rate constant is limited only by the collisional stabilization rate. By contrast subsequent oxidation is slow, requiring a high temperature for a sustained period. From a process control standpoint high temperatures and low pressures will serve the dual purpose of suppressing the homogeneous nucleation rate of (SiO)_x species while enhancing the oxidation rate of the clusters that are formed.

Reactions with H_2O . In calculating the influence of H_2O on the oxidation of silicon species, three reactions (SiH_2 , Si_2O_2 , $\text{Si}(\text{OH})_2$) have been calculated that involve very similar transition states but whose energetics are substantially different. In each case the lone pair in water interacts with the empty p orbital on the silicon atom. Summarized in Table 8 are the calculated activation energy, the heat of reaction, and the Mulliken charges on the Si, O, and H atoms involved in the reactions.

In keeping with a Polanyi type relationship for a homologous reaction series, there is an inverse correlation between the activation energy and the heat of reaction. Indeed, the transition state geometries are very similar as well. However, there is a substantial difference in activation energy between the insertion

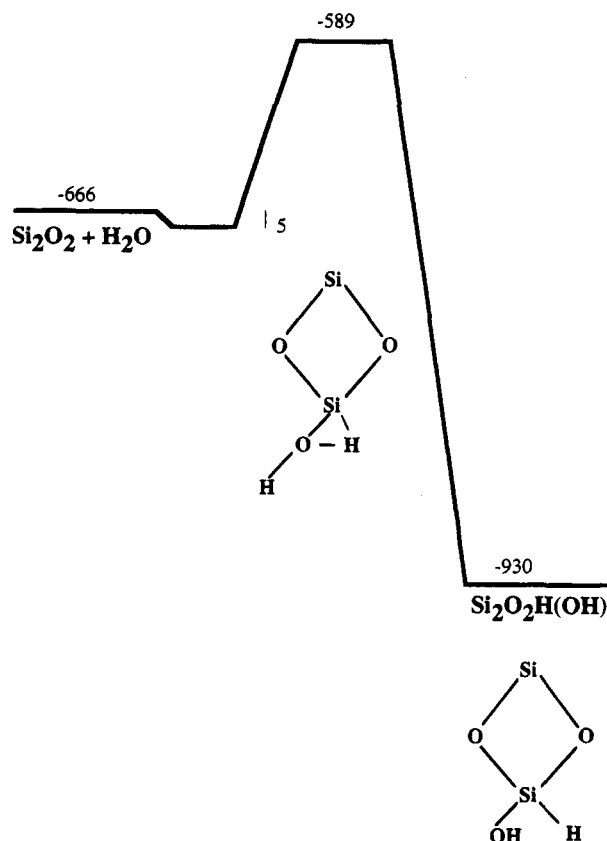


Figure 12. Energy diagram for $\text{H}_2\text{O} + \text{Si}_2\text{O}_2$.

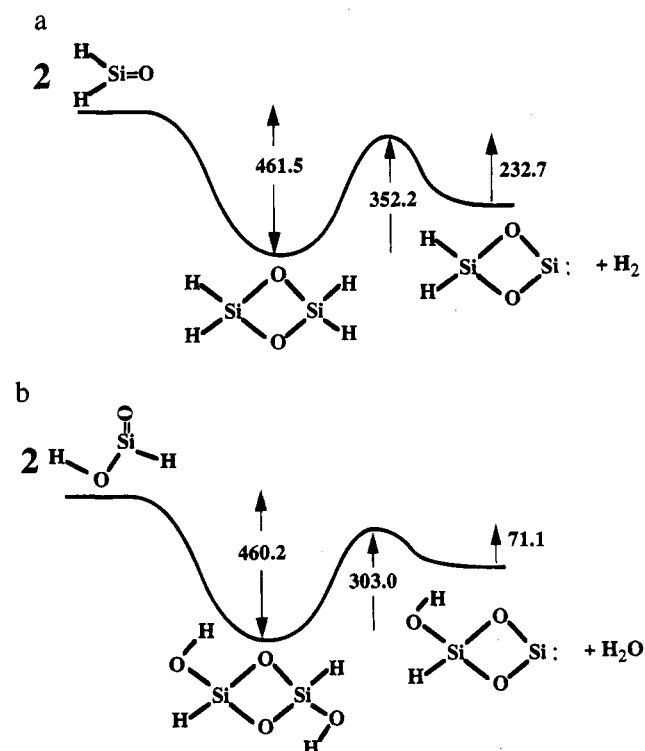


Figure 13. Energy diagram for dimerization of H_2SiO (a) and $\text{HSiO}(\text{OH})$ (b).

into SiH_2 and that for Si_2O_2 and $\text{Si}(\text{OH})_2$. Mulliken charge population analysis shows that the silicon has a net positive charge which does not change substantially between the reactant and the transition state, in keeping with the expectation that the transition state for an exothermic reaction reflects the properties of the reactant. Charge analysis shows that the SiH_2

TABLE 8: Oxidation of SiH_2 , Si_2O_2 , and $\text{Si}(\text{OH})_2$

species	Mulliken charge			E_a (kJ/mol)	ΔH_f (kJ/mol)	bond length (Å)	
	Si	O	H			Si-O	Si-H
H_2O		-0.87	0.43				
SiH_2	0.32						
$\text{SiH}_2 + \text{H}_2\text{O}$ (TST)	0.35	-0.88	0.34	3.1		1.87	1.62
H_3SiOH	0.90	-0.87	-0.17		76.2		
Si_2O_2	0.86						
$\text{Si}_2\text{O}_2 + \text{H}_2\text{O}$ (TST)	0.90	-0.87	0.36	16.9		1.82	1.63
$\text{Si}_2\text{O}_2\text{H}(\text{OH})$	1.30	-0.83	-0.15		64.9		
$\text{Si}(\text{OH})_2$	0.77						
$\text{Si}(\text{OH})_2 + \text{H}_2\text{O}$ (TST)	0.83	-0.86	0.33	19		1.85	1.62
$\text{HSi}(\text{OH})_3$	1.33	-0.85	-0.18		62		

reaction, which has the lowest barrier, also has the lowest net positive charge, while the other two reactions have both higher Si charge and activation barrier, with little difference between the two. The inserting oxygen atom in water shows no changes in atomic charge during the course of the reaction. It is the H atom on water that transitions from an electron donor to an acceptor, and the net charge transfer occurs between Si and H. The substantially larger insertion barrier into Si_2O_2 and $\text{Si}(\text{OH})_2$ over that for SiH_2 can be attributed to the higher electrostatic repulsion between the H and Si atoms.

Conclusions

Ab-initio molecular orbital calculations have been conducted on silicon oxy hydride equilibrium and transition state structures. A bond additivity correction procedure has been used to increase the accuracy of the calculations and to yield a list of heats of formation. The transition state results were used in subsequent RRKM/master equation calculations to give a set of pressure and temperature dependent rate coefficients. The calculations comprise what can be considered the beginning of a consistent set of thermochemical and kinetic data for modeling the combustion of silane in the presence of water. The results form a framework for analyzing the system for which there is a dearth of fundamental thermodynamic and kinetic information. This approach should prove to be a much more powerful conceptual and design tool than the possible alternatives: a complete empirical approach or an analogy to hydrocarbon systems. For example, SiO is much more reactive than CO . It is able to insert into a variety of other reactants and readily polymerizes. The fact that SiH_2 is the main intermediate in silane pyrolytic systems contrasts with the importance of methyl in methane decomposition. The poor π bonding nature of silicon relative to carbon makes the Si-O single bond favored over multiple bonds. The most clear example of this is that $\text{H}_2\text{Si}=\text{O}$ and its isomer HSiOH are of essentially equivalent energy, while in the carbon analog $\text{H}_2\text{C}=\text{O}$ is some 210 kJ/mol more stable than HCOH . The lower bond dissociation energies of Si-H bonds imply that $\text{Si}_x\text{H}_y\text{O}_z$ radicals are more stable than the parent species relative to the analogous carbon system, and as such more species in the silicon system will probably need to be accounted for in detailed chemical kinetic mechanisms.

The results indicate that SiH_2 which is the primary thermal decomposition product, will in the presence of H_2O insert to form hot silanol and be chemically activated to both H_2SiO and HSiOH and lesser amounts of H_3SiOH . Subsequent reaction with H_2O will lead to the silicon analog of formic acid at higher temperatures, which should rapidly polymerize. At lower temperatures the barrierless formation of silanediol would be favored. A number of thermal decomposition and radical attack reactions will tend to break species down to SiO and its hydrogenated analogs, which will at high temperature undergo shuffle reactions, the direction of which can only be known

from running simulations. In general, however, clustering can proceed through a number of species, as has been outlined, which must be subsequently oxidized to yield a Si/O stoichiometry of 0.5 for SiO₂. Indeed the gas phase formation of SiO₂ nanoparticles does not proceed by the nucleation of SiO₂ but rather by that of hydrated and hydrogenated analogs which are then subsequently oxidized through what would seem to be rate-limiting steps due to the high activation energies involved.

The results provide a thermodynamic and kinetic data base suitable for a systematic construction of a detailed chemical kinetic mechanism suitable for modeling combustion, chemical vapor deposition of silicon oxide films, and fine particle formation. Indeed it is the compilation of a reaction mechanism and its testing that are the only way to measure the sensitivity of the calculated rate constants and guide future experimental work.

Acknowledgment. The authors wish to acknowledge the contribution of Dr. Carl Melius of the Sandia National Laboratories for the many helpful discussions and access to and advise on using the BAC-MP4 methodology and software.

Supplementary Material Available: Compilation of calculated equilibrium and transition state geometries (12 pages). Ordering information is available on any current masthead page.

References and Notes

- (1) Ulrich, G. D. *Combust. Sci. Technol.* **1971**, *4*, 47.
- (2) Ulrich, G. D.; Subramanian, N. S. *Combust. Sci. Technol.* **1977**, *17*, 119.
- (3) Zachariah, M. R.; Chin, D.; Semerjian, H.; Katz, J. L. *Combust. Flame* **1989**, *78*, 287.
- (4) Kim, K.-S.; Pratsinis, S. E. *AIChE J.* **1988**, *34*, 912.
- (5) Zachariah, M. R.; Aquino, M. I.; Shull, R. D.; Steel, E. *Nanostruct. Mat.*, in press.
- (6) Hartman, J. R.; Famil-Ghiria, J.; Ring, M. A.; O'Neal, H. E. *Combust. Flame* **1987**, *68*, 43.
- (7) Darling, C. L.; Schlegel, H. B. *J. Phys. Chem.* **1993**, *97*, 8207.
- (8) Lucas, D. J.; Curtiss, L. A.; Pople, J. A. *J. Chem. Phys.* **1993**, *99*, 6697.
- (9) Darling, C. L.; Schlegel, H. B. *J. Phys. Chem.* **1994**, *98*, 8910.
- (10) Zachariah, M. R. Western States Section of the Combustion Institute, March, 1991.
- (11) Frish, M. J.; Head-Gordon, M.; Trucks, G. W.; Foresman, J. B.; Schlegel, H. B.; Raghavachari, K.; Robb, M. A.; Binkley, J. S.; Gonzalez, C.; DeFrees, D. J.; Fox, D. J.; Whiteside, R. A.; Seeger, R.; Melius, C. F.; Baker, J.; Martin, L. R.; Kahn, L. R.; Stewart, J.; Topiol, S.; Pople, J. A. *Gaussian 90*; Gaussian Inc.: Pittsburgh, PA, 1990.
- (12) Melius, C. F.; Binkley, J. S. Twenty-First International Symposium on Combustion, 1986, p 1953.
- (13) Schlegel, H. B. *J. Chem. Phys.* **1986**, *84*, 4530.
- (14) Benson, S. W. *Thermochemical Kinetics*; Wiley: New York, 1974.
- (15) Robinson, P. J.; Holbrook, K. A. *Unimolecular Reactions*; Wiley-Interscience: New York, 1972.
- (16) Tsang, W. *Combust. Flame* **1989**, *78*, 71.
- (17) Feng, Y.; Niiranen, J. T.; Bencsura, A.; Knyazev, V. D.; Gutman, D.; Tsang, W. *J. Phys. Chem.* **1993**, *97*, 871.
- (18) Zachariah, M. R.; Semerjian, H. G. *AIChE J.* **1989**, *35*, 2003.
- (19) Zachariah, M. R.; Joklik, R. G. *J. Appl. Phys.* **1990**, *68*, 311.
- (20) Zachariah, M. R.; Burgess, D., Jr. *J. Aerosol Sci.* **1994**, *25*, 487.
- (21) Zachariah, M. R. *Chem. Eng. Sci.* **1990**, *45*, 2551.
- (22) Raghavachari, K.; Chandrasekhar, J.; Gordon, M. S.; Dykema, K. *J. Am. Chem. Soc.* **1984**, *106*, 5853.
- (23) Gordon, M. S.; Pederson, L. A. *J. Phys. Chem.* **1990**, *94*, 5527.
- (24) Walch, S. P. *J. Chem. Phys.* **1993**, *98*, 3163.
- (25) Kudo, T.; Nagase, S. *J. Organomet. Chem.* **1986**, *253*, c23.
- (26) Tachibana, A.; Fueno, H.; Yamabe, T. *J. Am. Chem. Soc.* **1986**, *108*, 4346.
- (27) Kudo, T.; Nagase, S. *J. Phys. Chem.* **1984**, *88*, 2833.
- (28) Schaefer, H. F.; Frenking, G. *J. Chem. Phys.* **1985**, *82*, 4585.
- (29) Hastie, J. W.; Hauge, R. H.; Margrave, J. L. *Inorg. Chim. Acta* **1969**, *3*, 601.
- (30) Zachariah, M. R.; Carrier, M. D.; Blaisten-Barojas, E. Gas-Phase and Surface Chemistry in Electronic Material Processing. *MRS Symposium Proceedings*, 1994, Vol. 334, p 75.
- (31) Kudo, T.; Nagase, S. *J. Am. Chem. Soc.* **1985**, *107*, 2589.
- (32) Seidl, E. T.; Schaefer, H. F., III. *J. Am. Chem. Soc.* **1989**, *111*, 1569.

JP941438M